

# Parton Distributions and Event Generators

STEFANO CARRAZZA, STEFANO FORTE

Dipartimento di Fisica, Università di Milano and INFN, Sezione di Milano, Via  
Celoria 16, I-20133 Milano, Italy

JUAN ROJO

PH Department, TH Unit, CERN, CH-1211 Geneva 23, Switzerland

We present the implementation within the `Pythia8` event generator of a set of parton distributions based on NNPDF methodology. We construct a set of leading-order parton distributions with QED corrections, NNPDF2.3QED LO set, based on the same data as the previous NNPDF2.3 NLO and NNLO PDF sets. We compare this PDF set to its higher-order counterparts, we discuss its implementation as an internal set in `Pythia8`, and we use it to study some of the phenomenological implications of photon-initiated contributions for dilepton production at hadron colliders.

## 1. PDFs and event generators

The needs of physics at the LHC require an increasingly accurate control of the parton substructure of the nucleon: for example, this is a necessary ingredient in the accurate determination of Higgs couplings [1, 2], which in turn is essential both for precision determination of Standard Model parameters and for indirect searches for New Physics. Current sets of parton distributions [3] are based on increasingly refined theory, use an increasingly wide dataset (now also extended to LHC data) and attempt to arrive at an estimation of uncertainties which is as reliable as possible. An important ingredient in achieving all of these goals is the integration of parton distributions within Monte Carlo event generators [4]. Indeed, parton showering and hadronization are necessary in order to bridge perturbative QCD calculation with the quantities which are actually measured in experiments, all the more so as less inclusive observables are considered, even though also for observable which are in principle inclusive (such as the production of gauge bosons) comparisons are best made between theoretical predictions, and data collected in an experimental fiducial region.

Whereas next-to-leading (NLO) order Monte Carlo tools play an increasingly important role, leading-order (LO) Monte Carlo simulations are

still commonly used in a variety of applications. Furthermore, both LO and NLO Monte Carlo event generators typically rely on leading-order PDFs for the description of multiple-parton interactions and the underlying event, so that in fact generators which include a hadronization model, such as `Pythia` (and specifically its current version, `Pythia8` [5]) are tuned using one or more ‘native’ PDF sets

In this short contribution, we will discuss the NNPDF2.3QED LO PDF set, and its implementation within `Pythia8`: this is a PDF set which is based on the successful NNPDF methodology, which strives to minimize theoretical bias and construct statistically reliable parton distributions, recently used to produce a first global set of PDFs using LHC data, NNPDF2.3 [6]. This PDF set was subsequently used to construct a first set of PDFs with QED corrections and a photon distribution determined by experimental data, NNPDF2.3QED [7]. Recent general reviews of parton distributions are presented in Refs. [8, 9, 3].

## 2. The NNPDF2.3QED LO parton set

The NLO and NNLO NNPDF2.3QED PDF sets were recently presented in [7]. In these sets, the evolution of quark and gluon PDFs is consistently performed using combined QCD $\otimes$ QED evolution equations, and the photon PDF  $\gamma(x, Q^2)$  is determined from LHC vector boson production and deep-inelastic scattering data. In order to construct a corresponding leading-order set, NNPDF2.3QED LO, we start from the NNPDF2.1LO PDF sets [10], with two different values of  $\alpha_s(M_Z)$ : 0.119 and 0.130. Note that in Ref. [10] further LO sets were constructed, NNPDF2.1 LO\* in which the momentum sum rule was not imposed; however, this choice, sometimes advocated, did not turn out to be especially advantageous, hence we will not discuss these sets further.

The NNPDF2.3QED LO set is constructed by combining the PDFs from the NNPDF2.1 LO set with the photon PDF from the NNPDF2.3QED NLO set at  $Q_0^2 = 2 \text{ GeV}^2$ , and then evolving upwards this boundary condition with combined LO QCD $\otimes$ QED evolution equations, including  $O(\alpha_s)$  and  $O(\alpha)$ , but not  $O(\alpha\alpha_s)$  terms. This procedure (which clearly retains LO QED+QCD accuracy) is justified because of the very mild correlation between the photon and the other PDFs, and the large uncertainty on the photon PDF itself [7]. The set of PDFs thus obtained is then also evolved down to  $Q^2 = 1 \text{ GeV}^2$ : whereas leading-twist perturbative QCD might not be accurate in this region, low-scale PDFs are necessary for tunes of the underlying event and minimum bias physics in shower Monte Carlos.

The combined QCD $\otimes$ QED evolution has been performed with the `APFEL` package [11]. Among the various forms of the solution to the evolution

equation, differing by  $O(\alpha\alpha_s)$  terms which are beyond our accuracy, we use the so-called QECDS [11] solution, which was also used for the construction of the NNPDF2.3QED NLO and NNLO sets. Strict positivity of all LO PDFs has been imposed in the relevant range of  $x$  and  $Q^2$ .

In Fig. 1 we show the gluon PDF in the LO, NLO and NNLO NNPDF2.3QED fits. The much larger small- $x$  gluon is a well-known feature of LO PDF sets, due to the need to compensate for missing NLO terms when fitting deep-inelastic structure function data. It is an important ingredient for tunes of soft QCD dynamics at hadron colliders.

In Fig. 2 we also show the photon PDF at  $Q^2 = 10^4 \text{ GeV}^2$ , at LO, NLO and NNLO. The small differences seen arise due to the different evolution of quarks and gluons and their mixing with the photon through evolution equations.

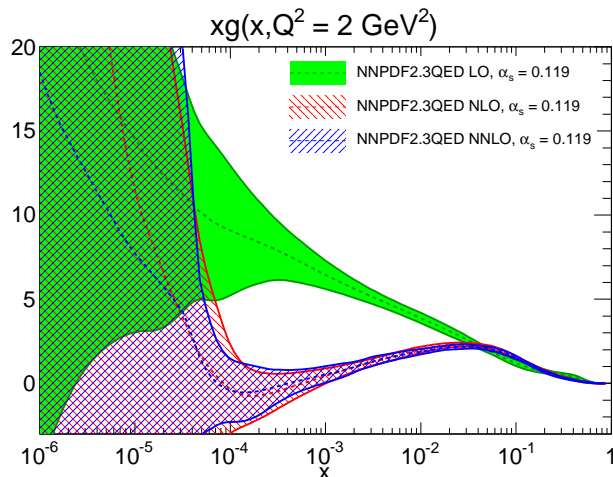


Fig. 1. The gluon PDF at LO, NLO and NNLO in the NNPDF2.3QED sets.

Finally, in Fig. 3 we compare the gluon PDF in the LO sets corresponding to the two different values of  $\alpha_s(M_Z) = 0.119$  and  $0.130$ : because of the slower running of  $\alpha_s$  at LO, the smaller value is more accurate at higher scale, and the larger value at low scales. Reassuringly, in the small  $x \leq 10^{-4}$ , relevant for tunes of soft physics at hadron colliders, the two sets turn out to agree within their large uncertainties.

### 3. Implementation in Pythia8 and phenomenological implications

The NNPDF2.3QED LO sets, with two different  $\alpha_s$  values, together with their NLO and NNLO counterparts, have been implemented as internal

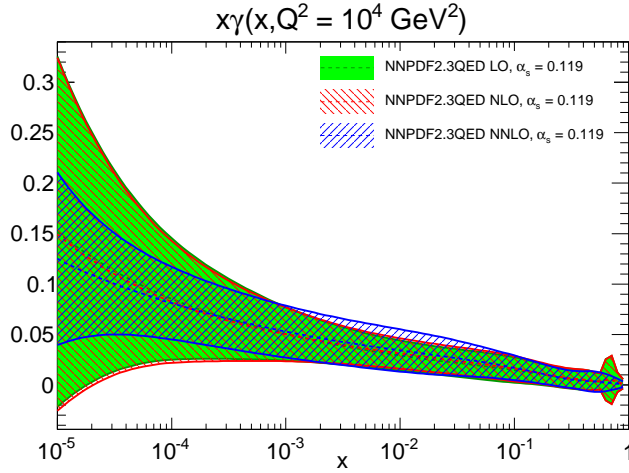


Fig. 2. The photon PDF at LO, NLO and NNLO in the NNPDF2.3QED sets.

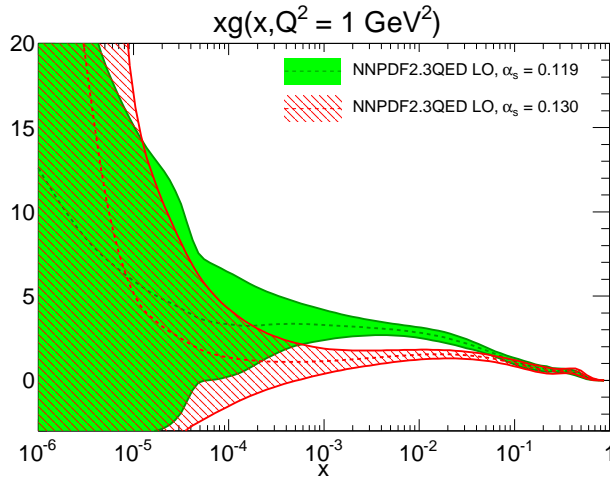


Fig. 3. The small- $x$  gluon PDFs in the NNPDF2.3QED LO set for  $\alpha_s = 0.119$  and 0.130.

PDF sets in `Pythia8` [5] starting with v8.180, and there is ongoing work by the `Pythia8` authors towards providing a complete new tune based on NNPDF2.3QED LO, including all the relevant constraints from LHC and previous lower-energy colliders [12].

For the time being, we will illustrate some of the phenomenological implications of the NNPDF2.3QED LO set by generating events with `Pythia8` for processes in which photon-initiated contributions are substantial. As a

case study, we consider dilepton production at the LHC 14TeV. Related studies were presented in the original NNPDF2.3QED paper [7] but were restricted to the parton level, while now we include the effects of the initial state parton shower and underlying event with the standard `Pythia8` tune. The QED shower option of `Pythia8` is turned off. We generate events for  $q\bar{q} \rightarrow \gamma^*/Z \rightarrow l^+l^-$  and for  $\gamma\gamma \rightarrow l^+l^-$ , and compare the relative contributions of the two different initial states. We consider both electrons and muons in the final state.

The invariant mass distributions of the dilepton pair at the LHC 14 TeV, without any kinematical cut, is shown in Fig. 4, in the  $Z$  peak mass region. We shown separately the contributions from the  $q\bar{q}$  and  $\gamma\gamma$  initiated subprocesses (though experimentally they cannot be separated, as they lead to the same final state). Is clear that in this region the  $q\bar{q}$  contribution is much larger, while the  $\gamma\gamma$  contribution is at the permille level. The total (leading order) cross section, including branching fractions, is found to be around 3.2 nb, in agreement with MCFM when run with the same input PDF set. We conclude that photon-initiated contributions are generally not required in the  $Z$  peak region, except perhaps for high precision studies, such as the determination of the  $W$  boson mass, where a permille accuracy in the distributions is required [13].

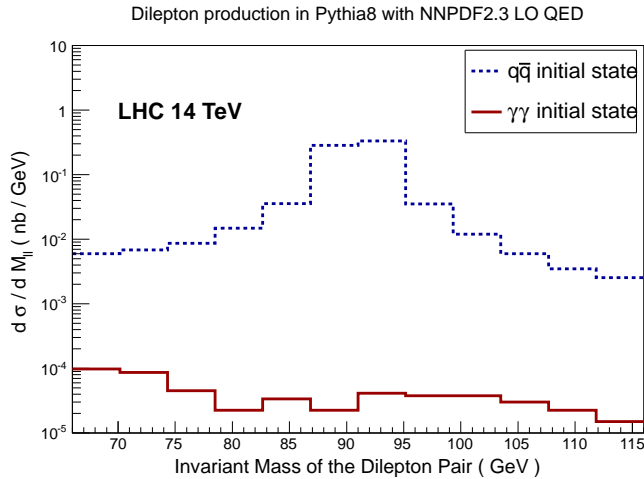


Fig. 4. Invariant mass distributions of the dilepton pair at the LHC 14 TeV, computed with NNPDF2.3QED LO and `Pythia8`. The contribution from the  $q\bar{q}$  and  $\gamma\gamma$  initiated subprocess are separately shown. No kinematical cuts have been applied.

The situation is quite different if we consider the high-mass tail. In Fig. 5

we show the region of dilepton invariant masses  $M_{ll}$  between 1 TeV and 2.5 TeV. We have applied realistic kinematical cuts based on the typical ATLAS and CMS acceptances, namely, we require  $p_{T,l} \geq 25$  GeV and  $|\eta_l| \leq 2.5$ . It is clear that now the photon-initiated contributions to the event yields are rather more significant, ranging from 10% at low masses to up to 50% at high masses. Therefore, photon-induced contributions are an important background for New Physics searches in electroweak production at high invariant masses.

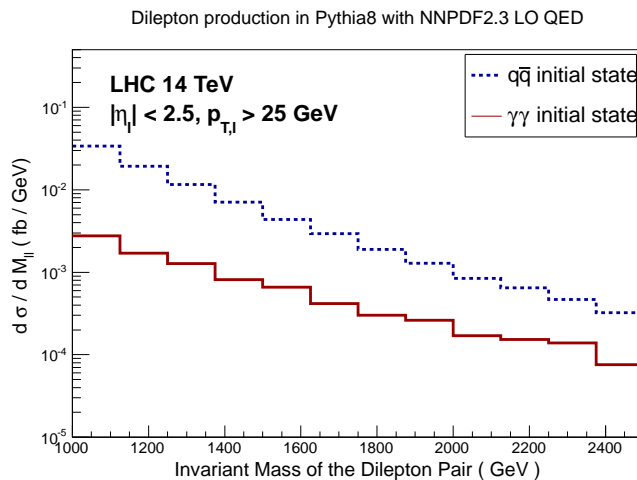


Fig. 5. Same as Fig. 4 but now in the high dilepton mass region. Realistic kinematical cuts have been applied to the events, see text.

In order to disentangle the two contributions, or to provide a measurement which is especially sensitive to the photon PDF, one may look at the rapidity distribution of the dilepton system. This is shown in Fig. 6 for fixed dilepton invariant mass of 2 TeV, at LHC 14 TeV, using the same kinematical cuts as before. It is clear that for a  $q\bar{q}$  initial state, the dilepton system tends to be produced more centrally (due to the  $s$ -channel exchange of the  $Z$  boson) while for a  $\gamma\gamma$  initial state, the system is more broadly distributed in rapidity ( $t$ -channel exchange). Indeed, for the bins with larger rapidity the contribution from  $\gamma\gamma$  diagrams becomes larger than that of  $q\bar{q}$  contributions.

All this suggest that a measurement of the rapidity distribution of high-mass Drell-Yan pairs, with a cut excluding the central region to enhance the  $\gamma\gamma$  contribution, might be a good way to isolate and eventually pin down the photon contribution to gauge boson production.

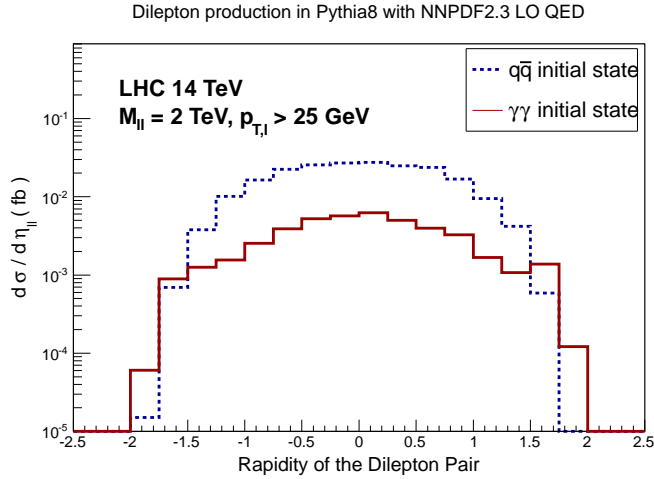


Fig. 6. The rapidity distribution of the dilepton system at LHC 14 TeV and for the same kinematical cuts as in Fig. 5.

#### 4. Using the NNPDF2.3QED LO sets

The NNPDF2.3QED LO sets can be obtained from the NNPDF website

<http://nnpdf.hepforge.org/html/nnpdf23qed/nnpdf23qed.html>

together with the corresponding C/C++ stand-alone code. They can be used together with the LHAPDF5.9.0 interface, and they will also be available in a future release of LHAPDF6. They are now also available as an stand-alone internal PDF set in Pythia8. For consistency of notation, the NNPDF2.1LO PDF set (without QED corrections) will henceforth be equivalently referred to as NNPDF2.3 LO.

**Acknowledgments:** We are grateful to T. Sjostrand and P. Skands for their help with the implementation of the NNPDF2.3 sets in Pythia8.

#### References

- [1] F. Petriello, *these proceedings*
- [2] D. Reuzzi, *these proceedings*
- [3] S. Forte and G. Watt, Ann. Rev. Nucl. Part. Sci. **63** (2013) 291 [arXiv:1301.6754 [hep-ph]].
- [4] A. Buckley, J. Butterworth, S. Gieseke, D. Grellscheid, S. Hoche, H. Hoeth, F. Krauss and L. Lonnblad *et al.*, Phys. Rept. **504** (2011) 145 [arXiv:1101.2599 [hep-ph]].

- [5] T. Sjostrand, S. Mrenna and P. Z. Skands, *Comput. Phys. Commun.* **178**, 852 (2008) [arXiv:0710.3820 [hep-ph]].
- [6] R. D. Ball, V. Bertone, S. Carrazza, C. S. Deans, L. Del Debbio, S. Forte, A. Guffanti and N. P. Hartland *et al.*, *Nucl. Phys. B* **867** (2013) 244 [arXiv:1207.1303 [hep-ph]].
- [7] R. D. Ball *et al.* [The NNPDF Collaboration], *Nucl. Phys. B* **877**, no. 2, 290 (2013) [arXiv:1308.0598 [hep-ph]].
- [8] A. De Roeck and R. S. Thorne, *Prog. Part. Nucl. Phys.* **66** (2011) 727 [arXiv:1103.0555 [hep-ph]].
- [9] E. Perez and E. Rizvi, *Rep. Prog. Phys.* **76** (2013) 046201 [arXiv:1208.1178 [hep-ex]].
- [10] R. D. Ball *et al.* [NNPDF Collaboration], *Nucl. Phys. B* **855**, 153 (2012) [arXiv:1107.2652 [hep-ph]].
- [11] V. Bertone, S. Carrazza and J. Rojo, arXiv:1310.1394 [hep-ph].
- [12] T. Sjostrand, *private communication*
- [13] G. Bozzi, J. Rojo and A. Vicini, *Phys. Rev. D* **83**, 113008 (2011) [arXiv:1104.2056 [hep-ph]].